



Research Article

Suppression of Polysulfide Dissolution and Shuttling with Diphenyl Disulfide Electrolyte for Lithium Sulfur Batteries

Chunhui Gao¹, Xueya Zhang³, Weiwei Sun¹, Huangxu Li^{2,*}, Qiyu Wang^{3,*}, Chunman Zheng^{1,*}

¹ College of Aerospace Science and Engineering, National University of Defense Technology, Changsha, China

² Department of Chemistry, City University of Hong Kong, Kowloon, Hong Kong, China

³ School of Metallurgy and Environment, Central South University, Changsha, China

E-mails: huangxuli2-c@my.cityu.edu.hk; wangqiyu@163.com; zhengchunman@nudt.edu.cn

Received: 12 December 2022; **Revised:** 4 January 2023; **Accepted:** 14 March 2023

Abstract: Lithium-sulfur (Li-S) batteries have been rising potential competitors in new battery technologies beyond lithium-ion battery, but the dissolution and shuttle of lithium polysulfide seriously deteriorate the cycling performance. Herein, we proposed diphenyl disulfide (DPDS) as the electrolyte additive for Li-S batteries. DPDS can interact with the discharge intermediate $S_2^{2-}/S_4^{2-}/S_6^{2-}$ ions, changing the stable form of lithium polysulfide in the electrolyte, inhibiting the shuttle of lithium polysulfide, and protecting the lithium anode. The initial discharge specific capacity of a Li-S battery with conventional electrolyte at 0.5 C is 1352.6 mAh/g, and the specific capacity of a Li-S battery with 200 cycles is 790.5 mAh/g. The initial discharge specific capacity of the battery containing 5.0 wt.% DPDS electrolyte at 0.5 C was 1296.3 mAh/g, and the capacity after 200 cycles was 899.9 mAh/g.

Keywords: diphenyl disulfide, electrolyte additive, lithium-sulfur battery, shuttle effect

1. Introduction

At present, lithium-sulfur (Li-S) battery has become one of the most promising new high-energy secondary batteries due to its high theoretical specific capacity (1675 mAh/g) and high theoretical energy density (2600 Wh/kg) [1–3]. Since the pioneering work by Nazar's group in 2009, proposing that confining S into a porous carbon host can improve the utilization and enhance the cycle life, the research on Li-S batteries has achieved rapid progress [4]. However, a suite of troublesome problems, severe polysulfide shuttle and sluggish redox kinetics, hinder the commercialization of Li-S batteries. The dissolution and shuttle of polysulfide not only cause the loss of active electrode materials, shorten the cycling life, but also enables the battery to have a high self-discharge rate [5–7].

In order to suppress the shuttle effect of lithium polysulfide, a large number of effective methods have been used, such as the design of porous cathode materials, the interlayer of blocks of lithium polysulfide, and the functional additive for electrolyte [8–10]. Wu et al. [11, 12] proved that the mercaptan-based additive biphenyl-4,4'-dithiol (BPD) could form a BPD-Sn complex with polysulfides, reducing the dissolution of polysulfides and inhibiting the shuttle effect. Gu et al. [13] found that adding carbon disulfide (CS_2) to the electrolyte could form a complex with polysulfide, which inhibits the migration of long-chain polysulfide to the Li anode. Yang et al. [14] added bis(4-nitrophenyl) carbonate (BNC) to the electrolyte, it can react with soluble polysulfide to generate insoluble polysulfides and by-products, which further react with lithium metal negative electrode to generate a

passivation layer with good lithium conductivity, and the low impedance of the passivation layer is conducive to improving the electrochemical performance of Li-S batteries. In addition, cobalt metallocene ($\text{Co}(\eta^5\text{C}_5\text{H}_5)_2$), [15] dithiothreitol (DTT) [16], N-methyl-N-ethylpyrrolidine (MEP+) cation [17], amino aniline trimer (ACAT) [18], glutamic acid [19], AlPO_4 [20] are functional additives that can effectively inhibit polysulfide shuttle.

The previous research of our research group found that the -S-R structure in sulfur-containing ether structure vulcanizing accelerator can interact with the S-S bond of lithium polysulfide, the high solubility lithium polysulfide can be transformed into S8 and $\text{Li}_2\text{S}/\text{Li}_2\text{S}_2$, which can reduce the sulfur content in the electrolyte and inhibit the shuttle effect [21]. DPDS contains -S-R structure, which is a common vulcanization accelerator, but its role as an electrolyte additive is not clear. Herein, we propose to use diphenyl disulfide (DPDS) as a functional additive to restrain the shuttling of lithium polysulfide, study the impact on the cycle and rate performance, and analyze its chemical reaction with lithium polysulfide and its action mechanism for Li-S battery.

2. Results and discussion

Figure 1(a) and Table S1 show the cycling performance at 0.5C and Coulombic efficiency (CE) of Li-S batteries with and without DPDS additive. The discharge specific capacity of different amounts (1.0 wt.%, 2.0 wt.%, 5.0 wt.%, 8.0 wt.%) of DPDS additives increased, especially the Li-S battery with 8.0 wt.% DPDS additive electrolyte shows an initial discharge specific capacity of 1474.7 mAh/g, and the second cycle still maintains a high specific capacity of 1402.0 mAh/g. The initial specific capacity of conventional electrolyte is also relatively high (1352.6 mAh/g), but the second cycle is reduced to 1117.7 mAh/g. The specific capacity of Li-S battery with conventional electrolyte drops rapidly in the first 10 cycles, and the capacity decay reaches 29.3%, the battery with 8.0 wt.% DPDS electrolyte attenuation rate is only 12.2%, and 5.0 wt.% DPDS electrolyte attenuation rate is 16.7%. After 180 cycles, the specific capacity 5.0 wt.% DPDS battery still maintains 985.5 mAh/g, while the conventional electrolyte battery only has 785.8 mAh/g. 8.0 wt.% DPDS battery has the highest specific capacity at the first cycle, but its capacity declines rapidly in the subsequent cycles. Considering comprehensively, we choose the 5.0 wt.% DPDS battery as the object of follow-up research.

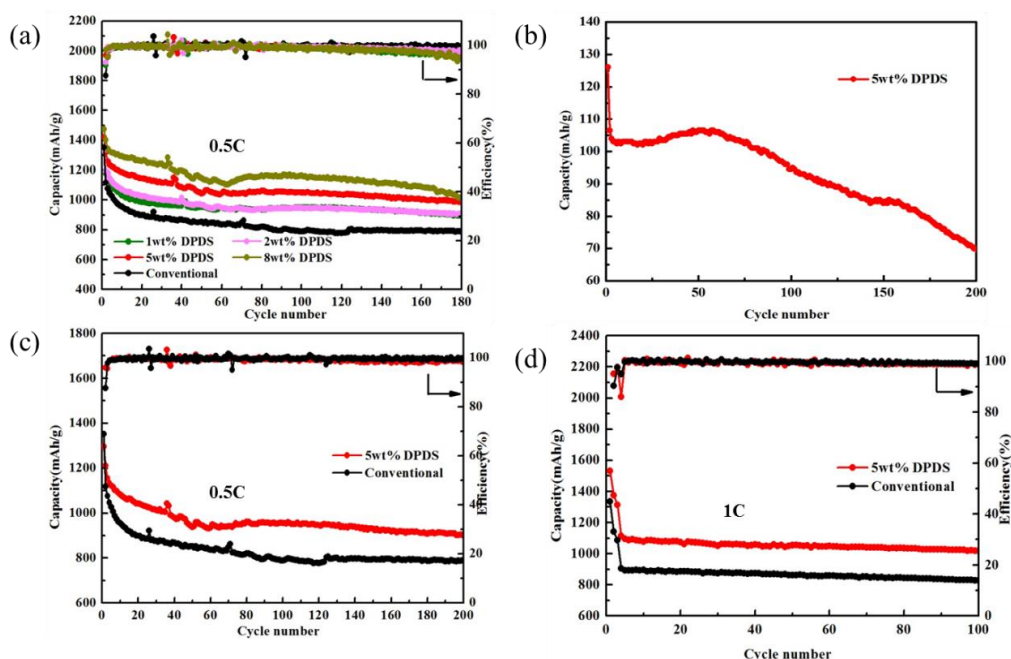


Figure 1. Cycling performance of Li-S batteries: (a) The batteries with different mass fractions of DPDS additive at 0.5 C; (b) The battery with 5.0 wt.% DPDS as electrolyte and sulfur-free carbon as cathode; (c) the batteries with conventional electrolyte and with 5.0 wt.% DPDS electrolyte deduct the capacity of additive at 0.5 C; (d) the batteries with conventional electrolyte and with 5.0 wt.% DPDS electrolyte at 1 C.

As the DPDS additive contains sulfur, it may provide some capacity, in order to deduct the capacity of the DPDS additive and show the true capacity of the battery, we use sulfur-free carbon as the cathode and 5.0 wt.% DPDS additive as the electrolyte to assemble the battery, its cycle performance as shown in Figure 1(b). It can be seen that DPDS can provide 70–130 mAh/g capacity, but it is unstable and decays quickly, which indicates that the S-S bond in DPDS can participate in the electrochemical reaction. Figure 1(c) shows the cycling performance

of 5.0 wt.% DPDS battery after deducting the capacity of DPDS additive, DPDS additive can significantly improve the stability of the Li-S battery, the specific capacity is still 899.9 mAh/g after 200 cycles and the capacity retention rate is 69.4%, while that of conventional electrolyte is 789.9 mAh/g and 58.4%, respectively. DPDS shows excellent electrochemical performance even at 1 C (as shown in Figure 1(d)), the specific capacity remained 1018.4 mAh/g after 100 cycles, while the conventional electrolyte was only 827.6 mAh/g.

Figure 2(a) shows the CV curves of Li-S batteries with different electrolytes. The CV curves of Li-S battery with conventional electrolyte consist of two reduction peaks and two oxidation peaks, corresponding to the discharge and charging processes respectively. In the first cycle, the reduction peak at 2.25 V corresponds to the reduction of sulfur to long-chain polysulfide, while the reduction peak at 2.0 V is due to the formation of short-chain $\text{Li}_2\text{S}_2/\text{Li}_2\text{S}$ [22, 23]. The two oxidation peaks of 2.42V and 2.47V formed in the anodic oxidation process correspond to the oxidation process of $\text{Li}_2\text{S}_2/\text{Li}_2\text{S}$ to intermediate lithium polysulfide and the conversion process of polysulfide to sulfur [16]. Compared to conventional electrolyte batteries, 5.0 wt.% DPDS electrolyte battery appears a new shoulder peak at 2.17 V, and the reduction of DPDS to polysulfide lithium at 2.09 V (as shown in Figure 2(b)). There is no simple superposition of the two reduction peaks, which indicates that DPDS is not a separate redox reduction but affects the entire electrochemical discharge progress. CV curves of 5.0 wt.% DPDS electrolyte batteries have a high coincidence at the first three cycles, it shows good reversibility compared to the conventional electrolyte battery. In addition, the areas of the oxidation peak and reduction peak are in direct proportion to the specific capacity, which means that the capacity contributed by DPDS as an active material is negligible compared with the entire specific capacity of Li-S batteries. Therefore, DPDS could reduce polarization and improve cycle reversibility by acting on the discharge process of Li-S batteries.

Figure 2(c, d) shows the charge and discharge curves of conventional and 5.0 wt.% electrolyte batteries. The first high voltage platform (2.3-2.4V) during the discharge progress represents the transformation of S to lithium polysulfide, and the second low platform (2.0-2.1V) represents the transformation of lithium polysulfide to $\text{Li}_2\text{S}_2/\text{Li}_2\text{S}$, and the voltage difference (ΔE) between the charge and discharge platforms represents the polarization voltage of the Li-S batteries. Compared with the polarization voltage of 204 mV of conventional electrolyte battery, the polarization voltage of 5.0 wt.% DPDS electrolyte battery is only 164 mV, which means that the DPDS additive can alleviate the polarization. In addition, DPDS reduced the Li_2S oxidation potential from 2.32 V to 2.13 V during the first cycle charge progress, accelerated the Li_2S oxidation reaction kinetics, and improved the reversibility of redox. Figure 2(e) shows the rate performance of Li-S batteries in conventional electrolyte and 5.0 wt.% DPDS electrolyte, the 5.0 wt.% DPDS electrolyte battery has better rate performance and reversibility. Figure 2(f) shows the Nyquist plots of Li-S batteries in conventional electrolyte and 5.0 wt.% DPDS electrolyte. The semicircle diameter of the 5.0 wt.% DPDS electrolyte battery is smaller, showing relatively small interface impedance, reflecting high interface compatibility between electrode and electrolyte. After 100 cycles, the interface impedance of the 5.0 wt.% DPDS electrolyte battery is relatively high, which may be due to the poor conductivity of the generation of discharge products in the electrochemical reaction.

To study the reaction mechanism of DPDS in Li-S battery, we have made the discharge visualization battery devices to observe the color change of electrolyte, the visualization experiment result as shown in Figure 3. In the conventional electrolyte (Figure 3(a, c)), with the increase of the discharge time at the high discharge voltage, the elemental S is continuously converted into lithium polysulfide, and the polysulfide in the electrolyte is continuously accumulated, so the color of the process from A to C is gradually deepened, showing a dark brown-red color; At the later stage of discharge, the color of electrolyte gradually becomes light and brown-yellow due to the transformation of polysulfide into insoluble $\text{Li}_2\text{S}/\text{Li}_2\text{S}_2$. In the discharge process of the battery containing DPDS additive (Figure 3 (b, d)), the color also experienced a process from dark to light (photo B-F in Figure 3(d)), but compared with the conventional electrolyte, the color of DPDS electrolyte is lighter, lighter brown and light yellow, indicating that the concentration of lithium polysulfide in the DPDS electrolyte was lower than that of the conventional electrolyte battery during the discharge process. It can be seen that the DPDS additive could prevent the dissolution of lithium polysulfide in the electrolyte during the discharge of the Li-S battery, which is beneficial to inhibit the shuttle effect.

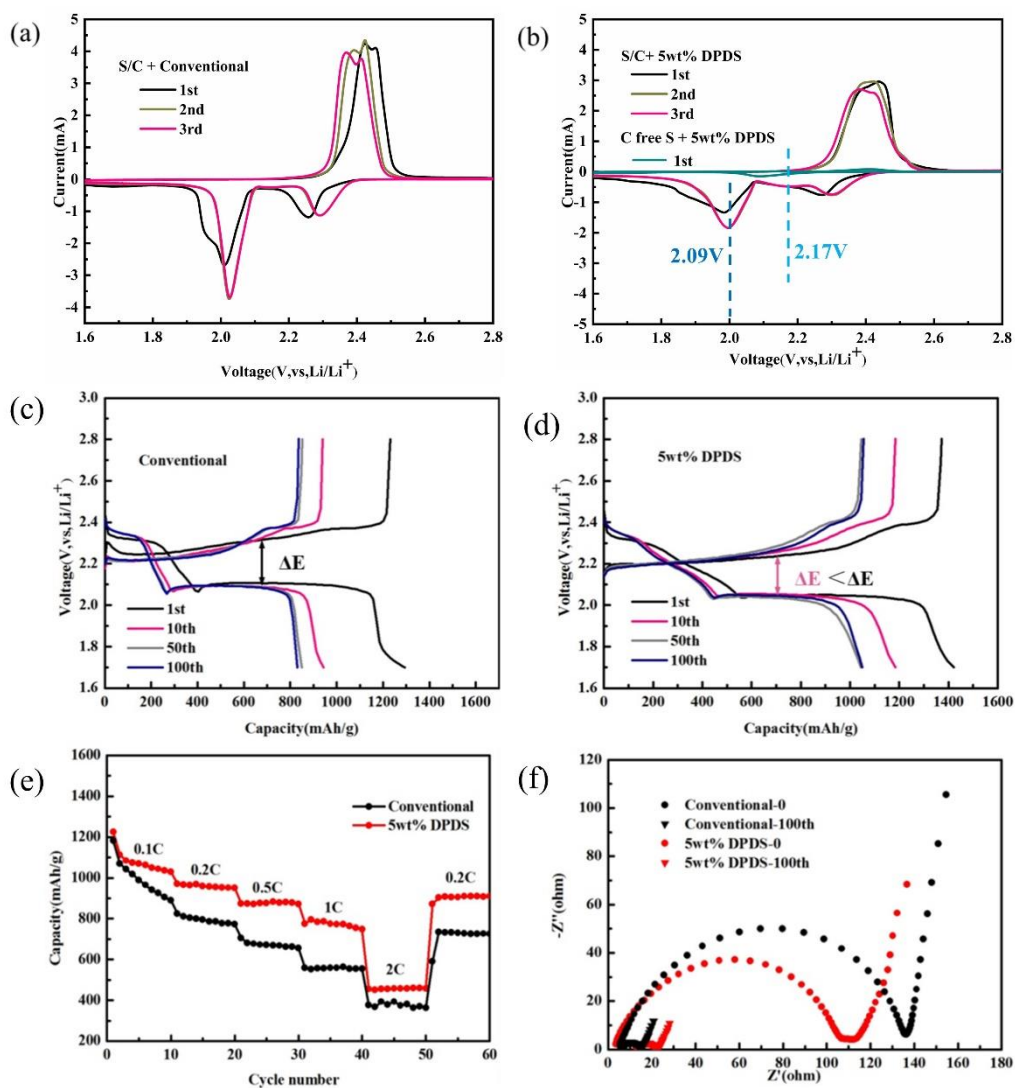


Figure 2. Cyclic voltammograms of Li-S batteries in the voltage range of 1.5–3.0 V at a scanning rate of 0.05 mV/s with (a) conventional electrolyte with S/C cathode, (b) 5.0 wt.% DPDS electrolyte with S/C cathode and S-free/C cathode; charge-discharge voltage profiles of Li-S batteries in (c) conventional electrolyte and (d) 5.0 wt.% DPDS additive electrolyte; (e) rate performance of Li-S batteries in conventional electrolyte and 5.0 wt.% DPDS electrolyte; (f) Nyquist plots of Li-S batteries in conventional electrolyte and 5.0 wt.% DPDS electrolyte.

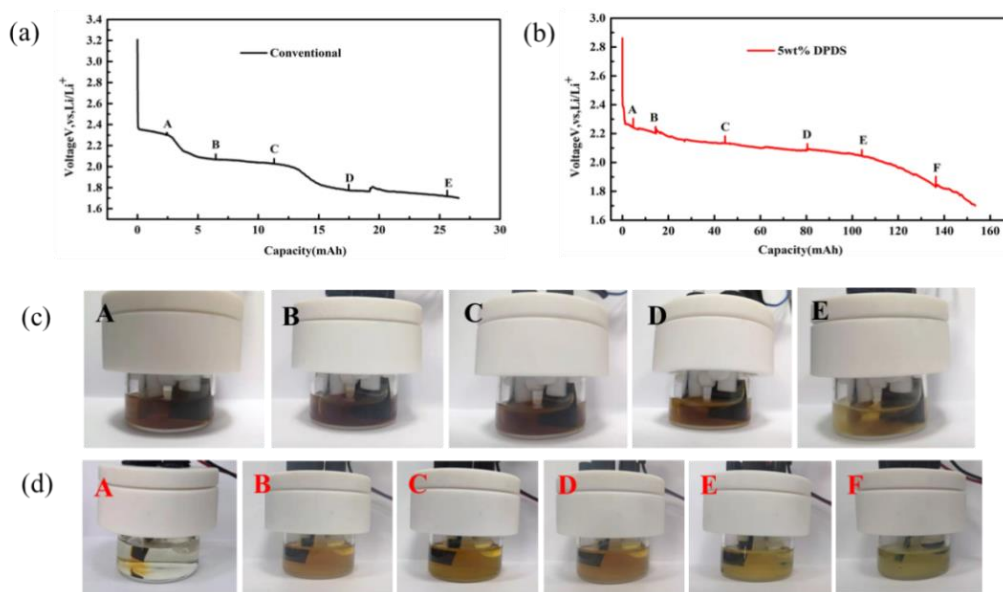


Figure 3. Visualization experiment of Li-S batteries at different discharge stages: discharge curves of batteries with (a) conventional electrolyte and (b) 5.0 wt.% DPDS electrolyte; color change of (c) conventional electrolyte and (d) 5.0 wt.% DPDS electrolyte at different discharge levels.

We believe that the reaction of DPDS with lithium polysulfide changes the stable form of lithium polysulfide in the electrolyte, thereby reducing the concentration of lithium polysulfide during battery discharge. To verify this conjecture, we add an equal amount of 20 mM Li_2S_6 to the conventional electrolyte and the 5 wt.% DPDS respectively to simulate the electrolyte environment during the discharge process, and observe the color change of the electrolytes, the pictures as shown in Figure 4((a) and (b)). Both the unreacted electrolytes are colorless and transparent (Figure 4(a)), after adding the Li_2S_6 solution (Figure 4(b)), the color of 5 wt.% DPDS electrolyte on the right side is lighter, indicating the chemical reaction of DPDS with Li_2S_6 . We tested the ultraviolet spectrum of Li_2S_6 without and with DPDS additive, the results are shown in Figure 4(c). Li_2S_6 solution has a shoulder peak at about 280 nm, corresponding to $\text{S}_4^{2-}/\text{S}_6^{2-}$ ions [24, 25], the shoulder peak at about 280 nm of Li_2S_6 solution with DPDS disappears and a new shoulder peak appears at about 230 nm, which is different from the characteristic peak of DPDS (at about 240 nm). It indicates that DPDS reacts with $\text{S}_4^{2-}/\text{S}_6^{2-}$ ions, reducing the content of $\text{S}_4^{2-}/\text{S}_6^{2-}$ ions, and producing new substances.

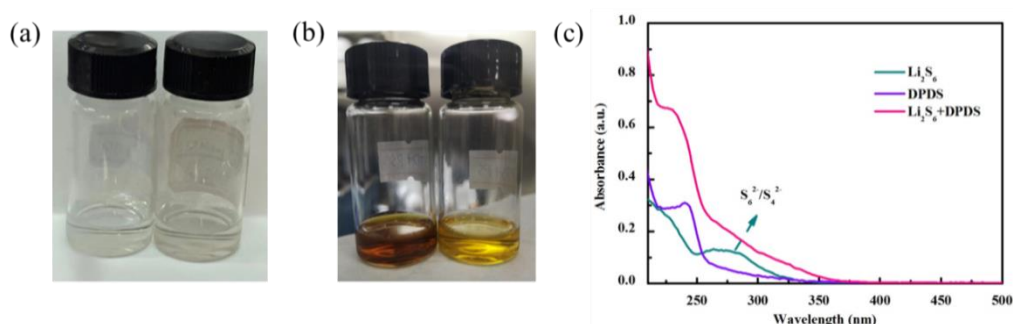


Figure 4. (a) digital photo of conventional electrolyte (left) and 5.0 wt.% DPDS electrolyte (right); (b) digital photo of conventional electrolyte + 20 mM Li_2S_6 (left) and 5.0 wt.% DPDS electrolyte + 20 mM Li_2S_6 (right); (c) ultraviolet spectrum of Li_2S_6 , DPDS, and Li_2S_6 +DPDS.

To explore the influence of DPDS additive on the anode, we tested SEM images in Li anode after 100 cycles in conventional electrolyte Figure S3((a) and (b)) and 5 wt.% DPDS electrolyte Figure S3((c) and (d)). In the conventional electrolyte, due to the dissolution and shuttle of polysulfides, side reactions occur on the Li anode, making the Li anode surface porous and loose, accompanied by the scattered accumulation of non-conduction species [11, 26]. However, in the 5 wt.% DPDS electrolyte, the surface of the Li anode is still smooth and dense. In addition, an XPS test was carried out on the Li anode cycling in conventional electrolyte and in the 5 wt.% DPDS electrolyte after 100 cycles, the results as shown in Figure S3(c). In conventional electrolytes, the peak at 169.0 eV ($\text{S } 2p_{3/2}$) represents the S-O bond in $-\text{SO}_2\text{CF}_3$, which is the product of the decomposition of LiTFSI salts [27, 28]. The peak at 167.0 eV ($\text{S } 2p_{3/2}$) represents thiosulfate, which is the product of lithium polysulfide oxidized by LiNO_3 [21, 29]. The two strong peaks at 161.7 eV and 160.5 eV indicate that the Li anode surface is covered with a large amount of irreversible Li_2S_2 and Li_2S [30], which is due to the polysulfides shuttle to the Li anode and have a side reaction with metallic Li. When 5.0 wt.% DPDS is added, the peaks at 161.7 eV and 160.5 eV drop sharply, which means that the amount of insoluble Li_2S_2 and Li_2S decreases. SEM images and XPS results show that the addition of DPDS additive effectively inhibits the shuttle effect of polysulfide.

3. Conclusions

In summary, we provide an effective additive to improve the cycle performance of Li-S batteries. DPDS additive can interact with discharge intermediate $\text{S}_4^{2-}/\text{S}_6^{2-}$, change the stable form of polysulfide in the electrolyte, reducing the content of $\text{S}_4^{2-}/\text{S}_6^{2-}$ significantly, and inhibiting the dissolution shuttle of lithium polysulfide. DPDS also reacts with metallic Li and generates insoluble substances such as $\text{Li}_2\text{S}_2/\text{Li}_2\text{S}$ through its reaction with polysulfide, for this reason, it can reduce the side reaction of Li anode and the accumulation of non-conductive species, to improve the stability of the Li anode. DPDS additive can increase the cycling performance of the Li-S battery, the initial specific capacity of the battery with conventional electrolyte at 0.5C is 1352.6 mAh/g, after 200

cycles the capacity is 790.5 mAh/g, and the capacity retention rate is 58.4%. By contrast, the initial specific capacity of the battery contains 5.0 wt.% DPDS at 0.5 C was 1296.3 mAh/g, after 200 cycles is 899.9 mAh/g, and the capacity retention rate was 69.4%, which was 11.0% higher than that of conventional electrolyte.

Conflicts and interest

There are no conflicts to declare.

Appendix

Experimental details

Preparation of sulfur-carbon (S/C) cathode

The melt diffusion method was used to produce the S/C composite used in this experiment. Sublimed sulfur (Aladdin) and porous carbon (Figure S1(a, c)) were mixed uniformly in a ratio of 6.5: 3.5 (mass ratio). The CS₂ solvent was added to the mixture, and the mixture was hand milling again until the CS₂ had completely evaporated. The mixture was placed in a sealed Teflon vessel at 160 °C for 12 h in an argon (Ar) -filled environment to obtain the S/C composite material (Figure S1(b, d)), EDS mapping proved the existence of sulfur (Figure S2). 80 wt. % S/C composite (65.0 wt. % S), 10 wt. % acetylene black and 10 wt. % polyvinylidene fluoride (PVDF) was dissolved in N-methyl-2-pyrrolidinone (NMP) to form a uniformly mixed slurry. The slurry with good uniformity was coated on an aluminum (Al) foil and dried under vacuum at 60 °C for 12 h to prepare the S/C cathode having S loading of 1.8–2.0 mg/cm². The S/C cathode was cut into disks with a diameter of 13 mm by a tablet press.

Preparation of electrolytes and lithium polysulfide (Li₂S₆)

The conventional electrolyte was 1 M lithium bis (trifluoromethane sulfonyl) imide (LiTFSI) and 2.0 wt. % LiNO₃ in a solvent of 1, 2-dimethoxyethane (DME)/1,3-dioxolane (DOL) (v/v = 1:1). In Ar-filled glove box, different amounts (1.0 wt. %, 2.0 wt. %, 5.0 wt. %, 8.0 wt. %) of diphenyl disulfide (DPDS, purchased from Bailingwei Science and Technology Co.) were added to the conventional electrolyte as the experimental electrolyte. The solution was stirred for 2 hours and stood for 12 hours to achieve a good dispersion of DPDS in the electrolyte. Add sublimed sulfur and lithium sulfide (Li₂S) into DME at a mass ratio of 80:23 to dissolve. The solution was sealed and stirred at 65 °C until it is completely dissolved to dark brown, which is a polysulfide (Li₂S₆) solution.

Preparation of button cells

The CR2025 button cells were assembled in a glove box with oxygen and water content less than 0.01 ppm and used for electrochemical detection. The S/C cathode and bare Cu foil as the working electrodes at the Li-S battery and Li-Cu battery, respectively. The Li foils were purchased from Alfa Aesar with a purity of >99.9% and as the counter electrode with a thickness of 700 μm. Polypropylene (PP2400, Celgard) is the separator, and the solution mentioned above is the electrolyte. The E/S ratio of the Li-S battery and Li-Cu battery is 20 μL/mgS and flooded, respectively. The assembly and testing of button cells are carried out at a temperature of 25 °C and pressure of 1 atmosphere.

Electrochemical measurements

The assembled Li-S battery and Li-Cu battery were allowed to stand for 12 h, and they were tested on a LANDAN test system (Wuhan, China). Before the CE test for Li-Cu batteries, the coin cells have an activation process, which is to use a small current density to cycle at 0-1V. Li was deposited onto Cu at 1 mA/cm² to a 1

mAh/cm² deposition capacity. The assembled Li–S batteries were allowed to stand for 12 h, after that they were charged and discharged at a potential of 1.7–2.8 V (vs. Li/Li⁺) on a LANDAN test system (Wuhan, China). Cyclic voltammetry (CV) measurements were performed on an electrochemical workstation (Solartron 1470 E) in a voltage range of 1.5–3.0 V (vs. Li/Li⁺) with a scan rate of 0.05 mV/s. Electrochemical impedance spectroscopy (EIS) measurements were conducted on an electrochemical workstation (Solartron 1470E), the frequency range operated 0.01Hz to 1 MHz and a voltage amplitude of 5 mV. All tests were accomplished at 25 °C.

Characterization

Li anodes were collected from recycled Li–S or Li–Cu coin cells, washed with fresh DME solvent to remove Li salts and dried in a glove box full of Ar. SEM observations and elements characterizations were obtained using scanning electron microscopy (SEM, FEI Nova Nano SEM) and energy dispersive spectrometer (EDS, attached to scanning electron microscopy). An FEI Tecnai TF20, Jeol 2100 equipped with an energy dispersive spectroscopy detector was used for the transmission electron microscopy (TEM) and elemental distribution analyses. The X-ray photoelectron spectroscopy (XPS) spectra were obtained by Thermo ESCALAB 250 spectrometer. The ultraviolet spectrum was characterized by U-4100 ultraviolet-visible near-infrared spectrophotometer (Hitachi, Japan)

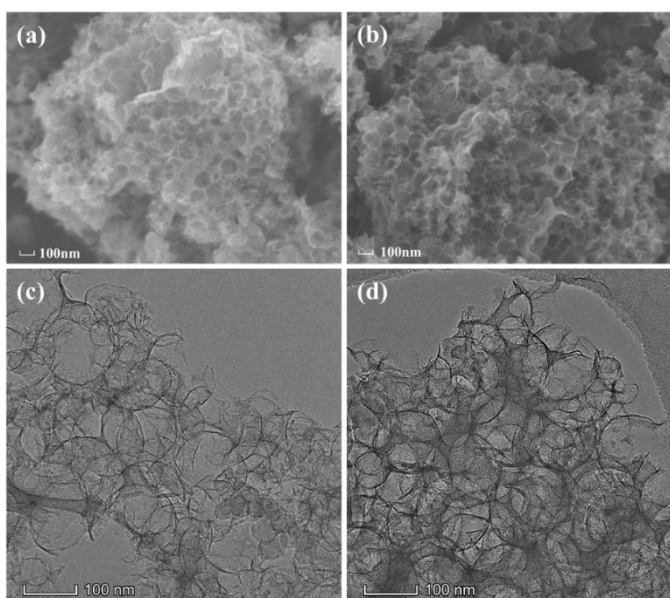


Figure S1. SEM images of (a) C and (b) S/C; TEM images of (c) C and (d) S/C.

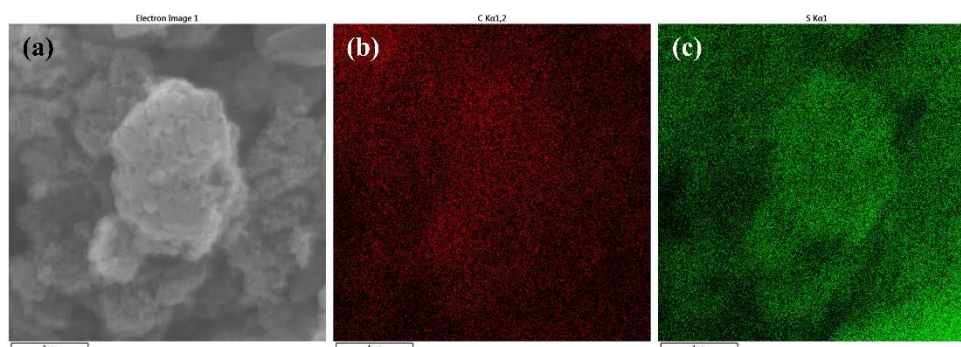


Figure S2. EDS mapping of S/C materials: (a) SEM; (b) C element; (c) S element.

Table S1. Cycling data of Li–S batteries with different mass fractions of DPDS additive at 0.5 C.

Batteries with different electrolyte	Initial Coulombic efficiency	First discharge specific capacity (mAh/g)	Specific capacity after 180 cycles (mAh/g)	Capacity retention after 180 cycles
Conventional Electrolyte	87.64%	1352.6	785.8	58.10%
1.0 wt.% DPDS	91.81%	1335.8	898.2	67.24%
2.0 wt.% DPDS	93.04%	1332.1	905.3	67.96%
5.0 wt.% DPDS	95.97%	1422.3	985.5	69.29%
8.0 wt.% DPDS	98.12%	1474.7	1010.2	68.50%

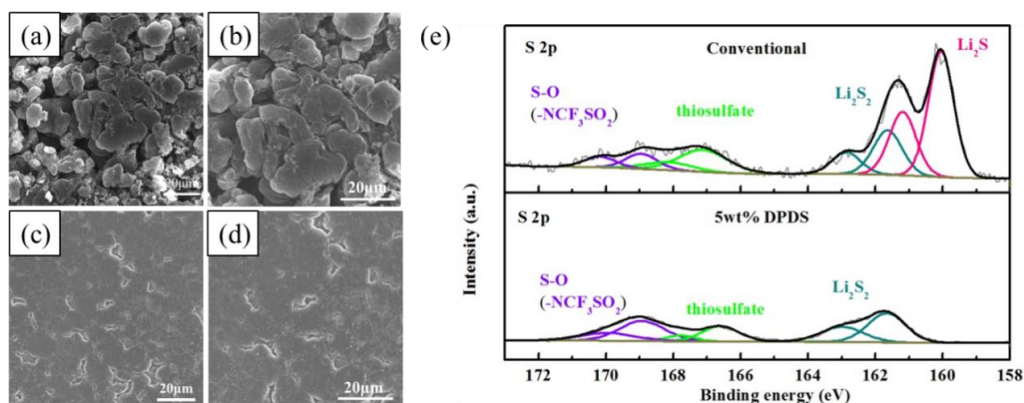


Figure S3. SEM images of Li anode surface after 100 cycles: (a, b) conventional electrolyte and (c, d) 5 wt.% DPDS electrolyte; (e) XPS spectrum of Li anode in conventional electrolyte and 5 wt.% DPDS electrolyte.

Acknowledgement

We thank the National Natural Science Foundation of China (No.52204324) and the China Postdoctoral Science Foundation (No. 2022M713878) for supporting this work.

References

- [1] Yang Y, Zheng G, Cui Y. Nanostructured sulfur cathodes [J]. *Chemical Society Reviews*, 2013, 42(7): 3018-3032.
- [2] Shi Z, Li M, Sun J, et al. Defect Engineering for Expediting Li-S Chemistry: Strategies, Mechanisms, and Perspectives [J]. *Advanced Energy Materials*, 2021, 11(23): 2100332.
- [3] Xu J, Liu K, Khan M A, et al. Sub-zero temperature electrolytes for lithium-sulfur batteries: Functional mechanisms, challenges and perspectives [J]. *Chemical Engineering Journal*, 2022, 443: 136637.
- [4] Ji X, Lee K T, Nazar L F. A highly ordered nanostructured carbon-sulphur cathode for lithium-sulphur batteries [J]. *Nature Materials*, 2009, 8(6): 500-506.
- [5] Zhang B, Wu J, Gu J, et al. The Fundamental Understanding of Lithium Polysulfides in Ether-Based Electrolyte for Lithium-Sulfur Batteries [J]. *ACS Energy Letters*, 2021, 6(2): 537-546.
- [6] Li G, Chen Z, Lu J. Lithium-Sulfur Batteries for Commercial Applications [J]. *Chem*, 2018, 4(1): 3-7.
- [7] Ren Y, Cui Z, Bhargava A, et al. A Self-Healable Sulfide/Polymer Composite Electrolyte for Long-Life, Low-Lithium-Excess Lithium-Metal Batteries [J]. *Advanced Functional Materials*, 2022, 32(2): 2106680.
- [8] Zhou L, Danilov D L, Eichel R-A, et al. Host Materials Anchoring Polysulfides in Li-S Batteries Reviewed [J]. *Advanced Energy Materials*, 2021, 11(15): 2001304.
- [9] Kim H, Kim C, Sadan M K, et al. Binder-free and high-loading sulfurized polyacrylonitrile cathode for lithium/sulfur batteries [J]. *RSC Advances*, 2021, 11(26): 16122-16130.
- [10] Elabd A, Kim J, Sethio D, et al. Dual Functional High Donor Electrolytes for Lithium-Sulfur Batteries under Lithium Nitrate Free and Lean Electrolyte Conditions [J]. *ACS Energy Letters*, 2022, 7(8): 2459-2468.

- [11] Wu H-L, Shin M, Liu Y-M, et al. Thiol-based electrolyte additives for high-performance lithium-sulfur batteries [J]. *Nano Energy*, 2017, 32: 50-58.
- [12] Singh A, Rafie A, Kalra V. Revisiting the use of electrolyte additives in Li-S batteries: the role of porosity of sulfur host materials [J]. *Sustainable Energy & Fuels*, 2019, 3(10): 2788-2797.
- [13] Gu S, Wen Z, Qian R, et al. Carbon Disulfide Cosolvent Electrolytes for High-Performance Lithium Sulfur Batteries [J]. *ACS Applied Materials & Interfaces*, 2016, 8(50): 34379-34386.
- [14] Yang T, Qian T, Liu J, et al. A New Type of Electrolyte System To Suppress Polysulfide Dissolution for Lithium-Sulfur Battery [J]. *ACS Nano*, 2019, 13(8): 9067-9073.
- [15] Kim K R, Lee K-S, Ahn C-Y, et al. Discharging a Li-S battery with ultra-high sulphur content cathode using a redox mediator [J]. *Scientific Reports*, 2016, 6(1): 32433.
- [16] Liu M, Chen X, Chen C, et al. Dithiothreitol as a promising electrolyte additive to suppress the “shuttle effect” by slicing the disulfide bonds of polysulfides in lithium-sulfur batteries [J]. *Journal of Power Sources*, 2019, 424: 254-260.
- [17] Chen Y, Zhang H, Xu W, et al. Polysulfide Stabilization: A Pivotal Strategy to Achieve High Energy Density Li-S Batteries with Long Cycle Life [J]. *Advanced Functional Materials*, 2018, 28(8): 1704987.
- [18] Chang C-H, Chung S-H, Han P, et al. Oligoanilines as a suppressor of polysulfide shuttling in lithium-sulfur batteries [J]. *Materials Horizons*, 2017, 4(5): 908-914.
- [19] Dong L, Liu J, Chen D, et al. Suppression of Polysulfide Dissolution and Shuttling with Glutamate Electrolyte for Lithium Sulfur Batteries [J]. *ACS Nano*, 2019, 13(12): 14172-14181.
- [20] Vu D-L, Kim N, Myung Y, et al. Aluminum phosphate as a bifunctional additive for improved cycling stability of Li-S batteries [J]. *Journal of Power Sources*, 2020, 459: 228068.
- [21] Xiang Q, Shi C, Zhang X, et al. Thiuram Vulcanization Accelerators as Polysulfide Scavengers To Suppress Shuttle Effects for High-Performance Lithium-Sulfur Batteries [J]. *ACS Applied Materials & Interfaces*, 2019, 11(33): 29970-29977.
- [22] Chen S, Dai F, Gordin M L, et al. Functional Organosulfide Electrolyte Promotes an Alternate Reaction Pathway to Achieve High Performance in Lithium-Sulfur Batteries [J]. *Angewandte Chemie International Edition*, 2016, 55(13): 4231-4235.
- [23] Pan H, Han K S, Vijayakumar M, et al. Ammonium Additives to Dissolve Lithium Sulfide through Hydrogen Binding for High-Energy Lithium-Sulfur Batteries [J]. *ACS Applied Materials & Interfaces*, 2017, 9(5): 4290-4295.
- [24] Barchasz C, Molton F, Duboc C, et al. Lithium/Sulfur Cell Discharge Mechanism: An Original Approach for Intermediate Species Identification [J]. *Analytical Chemistry*, 2012, 84(9): 3973-3980.
- [25] Zhang G, Zhang Z-W, Peng H-J, et al. A Toolbox for Lithium-Sulfur Battery Research: Methods and Protocols [J]. *Small Methods*, 2017, 1(7): 1700134.
- [26] Ma G, Wen Z, Jin J, et al. Enhanced performance of lithium sulfur battery with polypyrrole warped mesoporous carbon/sulfur composite [J]. *Journal of Power Sources*, 2014, 254: 353-359.
- [27] Agostini M, Xiong S, Matic A, et al. Polysulfide-containing Glyme-based Electrolytes for Lithium Sulfur Battery [J]. *Chemistry of Materials*, 2015, 27(13): 4604-4611.
- [28] Yang Y-b, Liu Y-x, Song Z, et al. Li⁺-Permeable Film on Lithium Anode for Lithium Sulfur Battery [J]. *ACS Applied Materials & Interfaces*, 2017, 9(44): 38950-38958.
- [29] Liang X, Kwok C Y, Lodi-Marzano F, et al. Tuning Transition Metal Oxide-Sulfur Interactions for Long Life Lithium Sulfur Batteries: The “Goldilocks” Principle [J]. *Advanced Energy Materials*, 2016, 6(6): 1501636.
- [30] Fan Q, Li B, Si Y, et al. Lowering the charge overpotential of Li₂S via the inductive effect of phenyl diselenide in Li-S batteries [J]. *Chemical Communications*, 2019, 55(53): 7655-7658.